STUDY OF THE BIODYNAMIC CHARACTERISTICS OF THE HUMAN HEAD

Jesse S. Ruan and Priya Prasad
Vehicle Systems Engineering
Ford Motor Company

ABSTRACT

A finite element model of an average adult human head was used to perform a modal analysis to characterize the intrinsic vibrational response of the human head. The first ten fundamental frequencies and associated mode shapes of the head were extracted by finite element analysis. Strain energy associated with the head's vibrational modes was plotted instead of mode shapes which become less meaningful for a complex structure such as the human head in three dimensional space. The effects on the vibrational response of the head were determined by carrying out a parametric study on the thicknesses and element types of the skull, brain with and without membranes, and the material properties of the CSF layer.

FOR SEVERAL DECADES, head trauma investigators have been trying to delineate the biodynamic characteristics of the human head by identifying its frequency response by both mechanical impedance tests and mathematical analysis. Mechanical impedance of a linear structure is defined by the ratio of exciting force to the resulting velocity of that structure. The resistive and reactive components of mechanical impedance of a linear system are the functions of frequency through resonances and antiresonances. Hence the natural frequency of a linear system can be found through the driving point impedance measurement of that system. Using driving point impedance test techniques, Gurdjian et al (1970) measured the natural frequency of a living head and a cadaver skull filled with silicon gel. They concluded that below 150 Hz the head moved essentially as a rigid body; and that 300 Hz was the first antiresonance mode and 880 Hz was the resonance mode. Along this line, Stalnaker et al (1971) measured the natural frequency of a human cadaver head as well as a monkey head *in vivo* and *in vitro*. Using Digital Fourier analysis techniques, Khalil and Viano (1979) measured the natural frequency of two dry cadaver skulls, one representing a 50th percentile male and another, a 5th percentile female head. They identified nine vibrational mode shapes and eleven natural frequencies for the male cadaver skull; five mode shapes and six frequencies for the female cadaver skull. Willinger and Cesari (1990) tested the natural frequency of three cadaver heads and one living head. Tzeng et al (1993) measured the natural frequency of the human head on seven healthy young male volunteers and identified the first three natural frequencies of the living head.

While experimental measurement has played a significant role on the human head natural frequency identification, mathematical modeling has also been involved in the investigation. Several analytical models represented by rigid shells filled with fluid have been proposed to study the free vibrational response of the human head (Engin and Liu, 1970, Misra and Chakravaty, 1982). These analytical models are very limited because they do not have an accurate geometry representation of the head and the dimensionless data yielded by these models are not useful in practice. A more versatile approach is Finite Element Analysis. Nickell and Marcal (1974) probably were the first ones to study the natural frequency of the human skull using the finite element method. They identified four fundamental frequencies for three different boundary conditions: rear support, frontal support, and base support. The natural frequencies of the human head found by finite element analysis have also been reported by other investigators (Ward and Thompson, 1975, Ruan et al, 1991, and Willinger et al, 1995).

Although modal analysis of the human cranial system using the finite element method has been reported by many investigators, the *frequency response* of the human head is still not clearly shown. Nickell and Marcal's (1974) study involved only the skull, and Ward and Thompson's (1975), only the brain. Ruan's et al (1991) study was based on a two-dimensional model. In recent years, several reports concerned with the vibrational characteristics of the human head using both finite element and lumped-spring-mass approaches were published (Willinger and Cesari, 1990, Willinger et al, 1992, 1995). These authors concluded that at a frequency of 200 Hz, the brain and skull moved as a solid body, but beyond this frequency the skull and the brain were decoupled; hence relative movement between the brain and skull occurred (Willinger and Cesari, 1990). Based on this conclusion, a lumped-spring-mass model was proposed to study brain tolerance in frequency field (Willinger and Cesari, 1991) and a Bimass Dummy Head was devised and proposed to experimentally measure the relative motion between the brain and skull (Willinger et al, 1993).

These studies are valid attempts to characterize the dynamic response of the human cranial system, but the "Bimass Dummy Head," based on the analysis of a lumped-spring-mass model may be too simplistic to measure the relative motion between the brain and skull. It likely will create spurious brain-skull relative displacement because the lumped-spring-mass model is inadequate to simulate brain-skull relative motion during head impacts. While it is still not clear whether the "decoupled" phenomenon between the brain and skull exists in certain frequency ranges, the frequency response of the human cranial system is worth further investigation.

In this study, a finite element model of a 50th percentile human head was used to perform a modal analysis to characterize the frequency response of the human head. The influence on the frequency response of the cranial system was also studied by varying the thickness of the skull, the material properties of the cerebral spinal fluid (CSF), and using different types of elements to simulate the skull. The dynamic behavior of the human head is discussed, based on the analysis results and previous studies of finite element head impact.

METHODS

The natural frequency of a mechanical structure of the head can be mathematically depicted by either a lumped-spring-mass model or a finite element model. Which approach is more appropriate depends on the desired degree of approximation and the complexity of the mechanical system. The lumped-spring-mass model is inadequate to simulate the dynamic characteristics of the human cranial system. Therefore, in this study, the finite element method was chosen. The finite element model represents an average adult head and incorporates most of the anatomical features of the human head. Figure 1 shows a three-dimensional view of this model which has been used previously for head impact study (Ruan et al, 1993, Ruan and Prasad, 1994). The skull was modeled in details, including three layers (outer table, diploe, and inner table) and the foramen magnum. The depressions and ridges of the base or floor of the cranium were taken into account by modeling three fossae, from the most superior to the most inferior, anterior fossa, middle fossa, and posterior fossa as shown in Figure 2. The cerebral spinal fluid (CSF) creates a cushion layer between the brain and inner table. It was modeled as brick elements. The dura firmly attaches to the inner surface of the inner table and was modeled as membrane elements. The falx separates the brain into left and right hemispheres and it

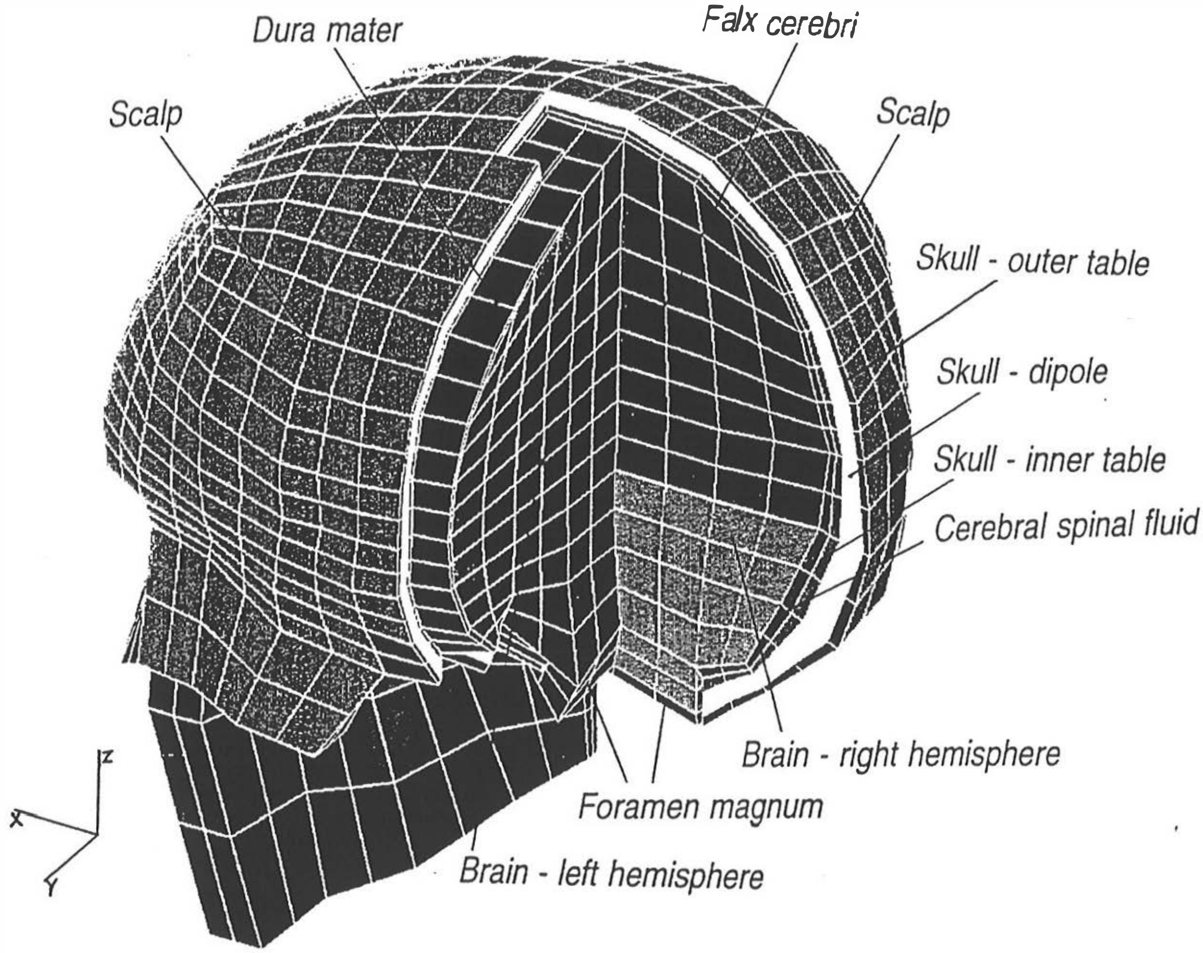

Fig. 1 Three-dimensional view of the human head finite element model

Table 1 Material Properties of Head Tissues

Head tissue element type in ( )	Young's Modulus (E, kPa)	Poisson Ratio (ν)	Mass Density (ρ, kg/m³)
Outer table (solid)	5.465 X 10^6	0.22	3000
Diploe (solid)	2.684 X 10^6	0.22	1750
Inner table (solid)	5.465 X 10^6	0.22	3000
CSF (solid)	1.485 X 10^2	0.485	1040
Brain (solid)	5.58 X 10^2	0.499	1040
Dura mater (membrane)	3.15 X 10^4	0.45	1130
Falx (membrane)	3.15 X 10^4	0.45	1130
Scalp (membrane)	1.672 X 10^4	0.42	1300

was also modeled as membrane elements (Figure 1). The size of the model contains 6080 nodes, 5456 solid elements, and 1895 membrane elements.

The material properties and element types of the baseline model are listed in Table 1. These parameters were adopted from the previous study since the model has shown good agreement between model responses and experimental data during head impacts (Ruan et al, 1993).

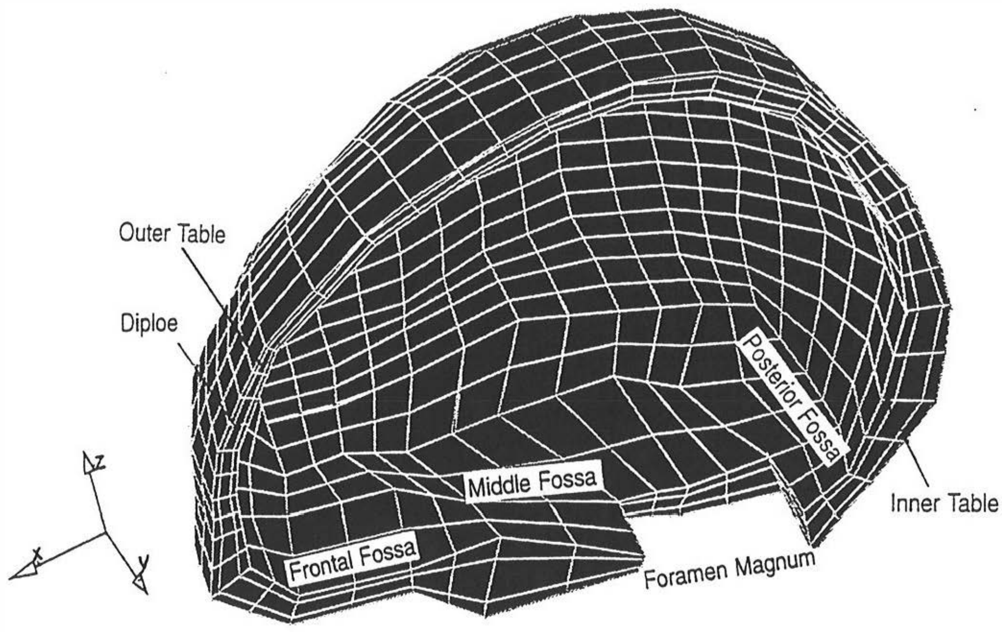

Fig. 2 The depressions and ridges of the floor or base of the cranium

In order to study the effects on the frequency response of the human cranial system, the natural frequencies of the skull and brain were first extracted separately from the baseline model and then from the full head. The skull was also simulated by shell elements to find out the effects of element type and skull thickness on the skull frequency response. The material properties of the CSF layer between the skull and brain was varied to study the effect of this boundary layer on the frequency response of the full head.

The boundary conditions were applied at the atlano-occipital joint area. The nodes surrounding the foramen magnum were fixed, since the skull was supported by the articular surfaces of the 1st cervical vertebra. Supports at other locations of the head are not considered because the data generated with other boundary conditions have less practical meaning for a living head. When the neck was included in the study, the boundary conditions were applied at the lower end of the neck. The neck was modeled as brick elements for the vertebra and the spinal fluid, and as membrane elements for the dura surrounding the spinal cord.

The numerical approach to solving for natural frequency is the Lanczos method. This method combines the transformation and the tracking methods to extract real roots (eigenvalues) of the eigenvalue problem. In comparison with other methods (Givens method, Householder method, and Inverse Power method), the Lanczos method computes accurate eigenvalues and eigenvectors and does not miss roots. It is efficient for many modes extraction and for large-sized problem.

RESULTS

The frequency responses of the skull and brain were first studied separately from the baseline model. The skull was simulated by shell elements and the thickness of the shell elements was varied to study the effects of element type and skull thickness on the vibrational response of the skull. Since the thickness of the skull was not uniform for a solid skull (baseline model), its average thickness (6.2 mm) was used for a shell skull and this value was increased by 33% for a thicker shell skull, to 8.25 mm. The brain was simulated with and without membranes (dura mater and falx cerebri) to study the effect of membranes on the frequency response of the human brain. Ten fundamental frequencies and associated mode shapes were extracted. Table 2 lists the natural frequencies of the human skull and brain computed from the analysis.

Figure 3 shows a frequency bar chart for the isolated skull when it was simulated by solid elements averaging 6.2 mm thick and shell elements with thickness of 6.2 and 8.25 mm. The natural frequency from the shell element simulation was about 70% of that from the solid element simulation for the first two modes, but little difference was shown for the higher modes (3 to 10). When the thickness of the skull was increased by 33% in the shell element simulation, skull frequencies were increased by about 30% for the first two modes but less than 10% for the higher modes (3 to 10). Skull frequencies computed in this study are lower than those obtained by Khalil and Viano's (1979) dry cadaver skull study. They reported eleven frequencies ranging from 1385 to 4792 Hz for the male cadaver skull and six frequencies from 1641 to 5000 Hz for the female cadaver skull. Nickell and Marcal (1974) reported skull frequencies based on finite element analysis ranging from 68 to 807 Hz for rear support, 86 to 864 Hz for frontal support, and 194 to 1327 Hz for base support. Taking into account that Nickell and Marcal used triangle elements with a lower Young's modulus and we used quadrilateral elements with a higher Young's modulus, the frequencies between these two are comparable for the base support condition.

Table 2 Natural Frequency of Human Skull and Brain (Hz)

Mode	Skull (solid) (t=varied)	Skull (shell) (t=6.2mm)	Skull (shell) (t=8.25mm)	Brain (w/o membrane)	Brain (w membrane)
1	325	217	254	4	15
2	378	258	294	5	24
3	993	719	785	6	39
4	1020	726	807	18	42
5	1735	1308	1430	25	66
6	1766	1311	1480	31	76
7	1891	1347	1609	62	110
8	2064	1585	1755	63	117
9	2100	1592	1815	71	125
10	2167	1626	1861	78	129

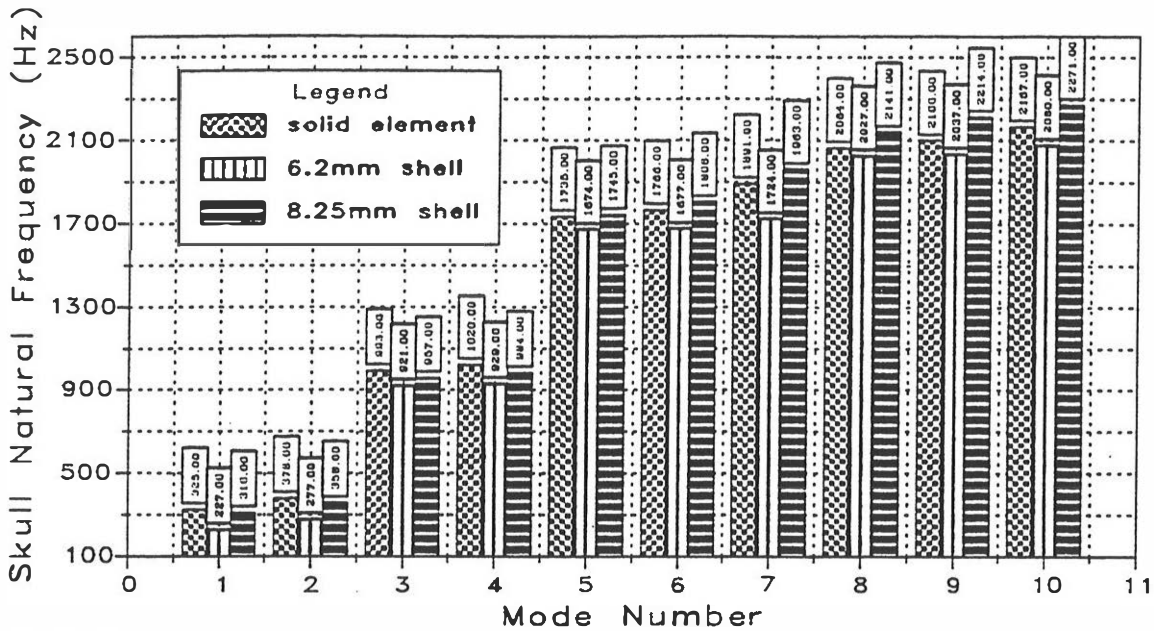

Fig.3 Frequencies of the skull for different element types and thicknesses

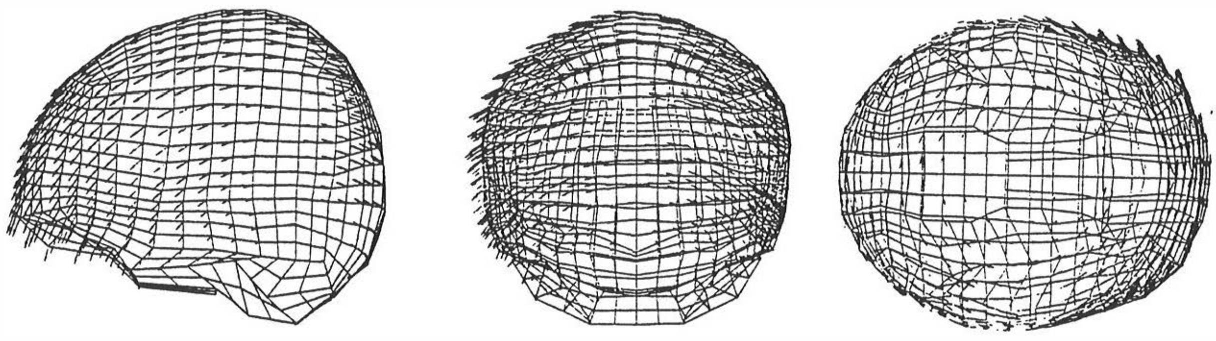

First mode - side view | Second mode - front view | Third mode - top view

Fig.4 Vector plots of the first three mode shapes of the human skull

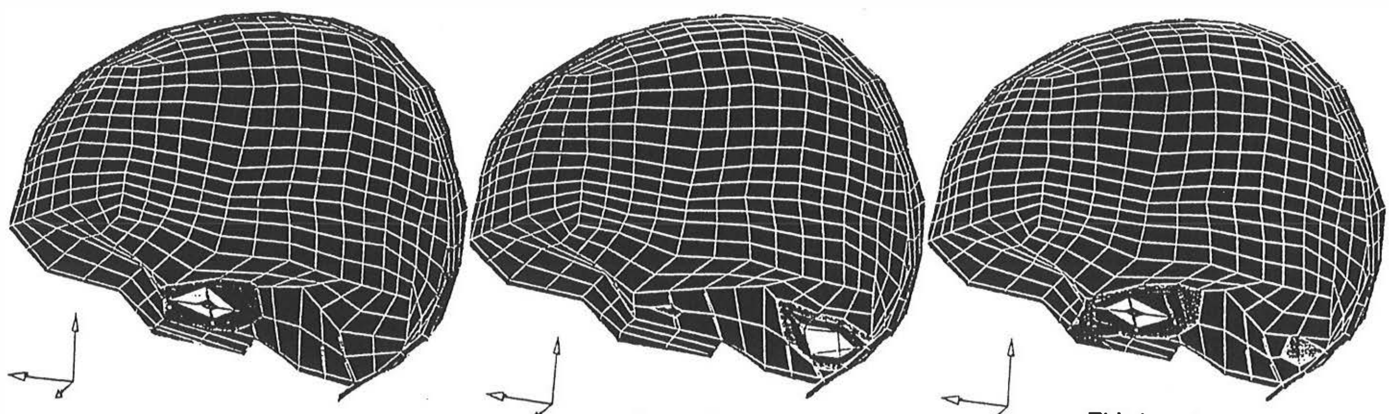

First mode | Second mode | Third mode

Fig.5 Strain energies of the first three mode shapes of the isolated skull

The mode shapes involved local modes and became highly complicated in three dimensional space with higher modes. Only the first three mode shapes are shown in the vector plot in Figure 4. As can be seen in this figure, the first mode shape rotated about the lateral axis (y-axis), the second mode rotated about the anterior-posterior axis (x-axis), and the third mode rotated about the superior-inferior axis (z-axis). Figure 5 shows strain energy of the skull for the first three modes. Large strain energy was always shown in the base of the cranium. In modes 8 and 10, large strain energy was also shown in the parietal-occipital bone area.

As can be seen in Table 2 as well as in Figure 6 -- a frequency bar chart of the isolated brain with and without interior membranes (dura mater and falx) -- the isolated brain possesses a very low frequency and its frequency response was affected greatly by the dura and falx. The same conclusion has been pointed out by Ward and Thompson (1974) who reported the natural frequency of the brain with and without membranes to be 23 and 19 Hz, and by Ruan et al (1991) who reported five brain frequencies ranging from 48 to 89 Hz without membranes and 72 to 119 Hz with membranes. Figure 7 shows the strain energy of the isolated brain for the first three modes. Large strain energy was always shown in the brain stem area even with the higher mode shapes. In modes 7 to 10, large strain energy was also shown in the white matter and in the corpus callosum.

The frequency response of the full head was studied in several cases. In the baseline model, the Young's modulus of the CSF was increased by factors of 2 and 10, and also to the value of the skull inner table. The interior membranes were excluded in the baseline model; and baseline model included the neck. The frequencies of the head in these cases are shown in Table 3. Figure 8 shows the frequency bar chart of the head for these different cases. When the Young's modulus of the CSF was increased by factors of 2 and 10, and then to the value of that of the inner table, head frequency increased by 3%, 6%, and 8%. Figures 9 and 10 show the strain energy of the skull and brain, respectively, for the first three modes of the baseline model. As in the isolated skull case, large strain energy occurred in the floor of the skull of the baseline model as seen in Figure 9. Large strain energy of the brain occurred in the occipital lobe, and in the occipitotemporal area as seen in Figure 10. In the higher modes (mode 4 and up), large strain energy appeared in the white matter and in the corpus callosum.

Table 3 Natural Frequency of the Human Head (Hz)

Mode	Baseline	2XCSF	10XCSF	CSF=Inner T	w/o mem.	with Neck
1	154	158	161	163	132	91
2	157	162	167	167	136	97
3	159	163	168	173	138	140
4	173	180	186	188	159	160
5	184	190	195	199	164	163
6	189	195	199	201	167	173
7	190	195	200	203	170	182
8	195	201	204	211	175	185
9	197	202	208	212	176	190
10	198	203	209	219	181	195

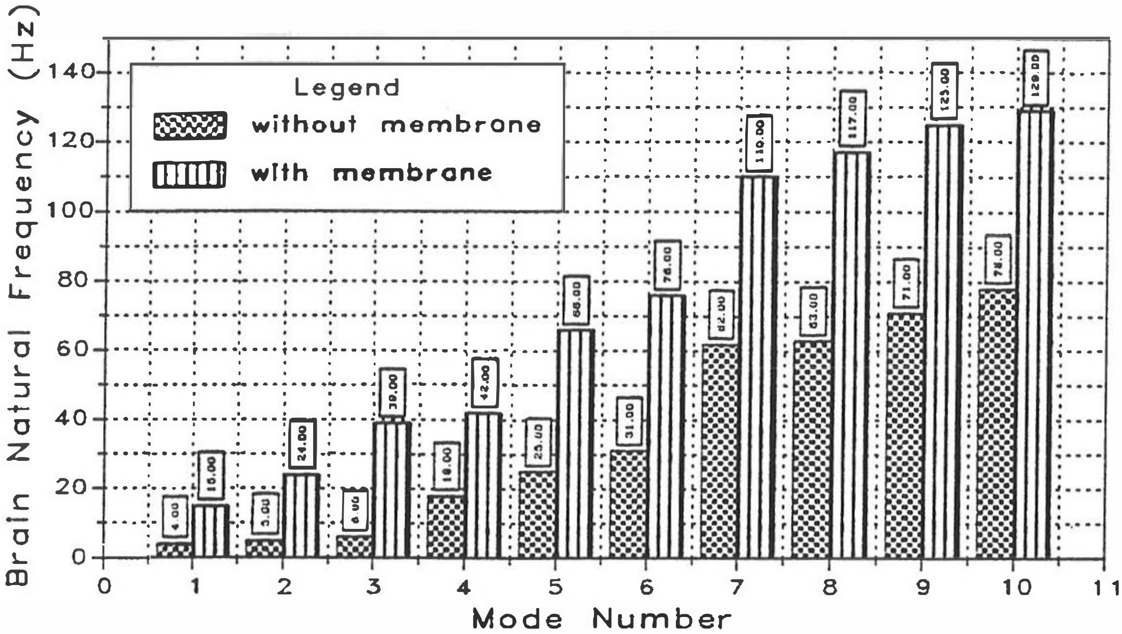

Fig.6 Frequencies of the isolated brain with and without membranes

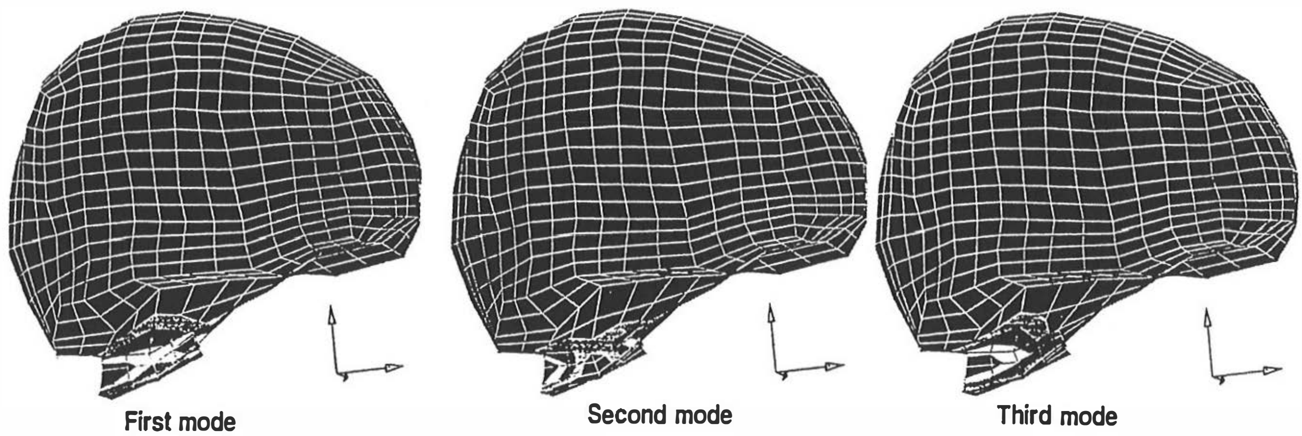

Fig.7 Strain energies of the first three mode shapes of the isolated brain

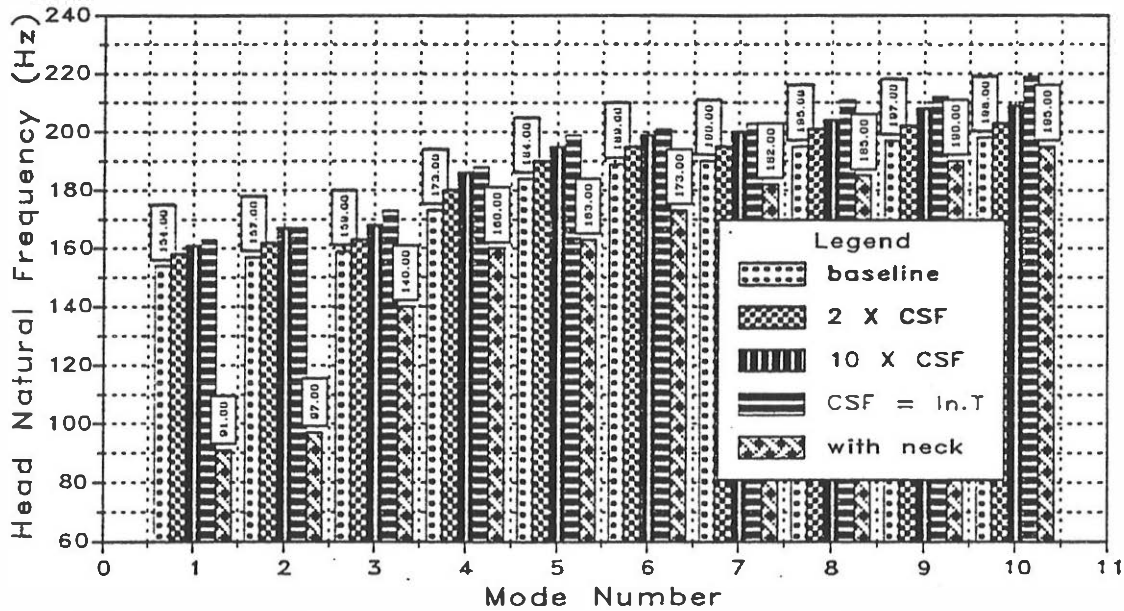

Fig.8 Frequencies bar chart of the human head in different conditions

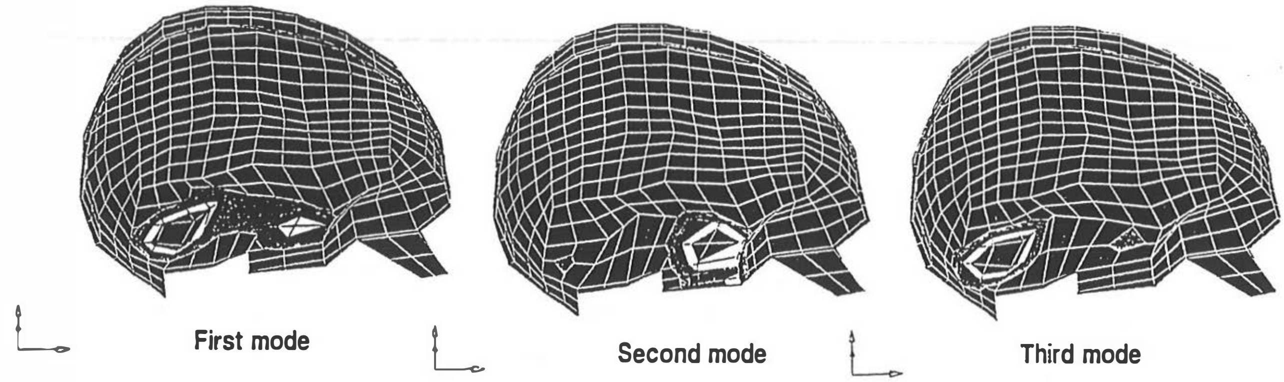

Fig.9 Strain energies of the first three mode shapes of the human skull

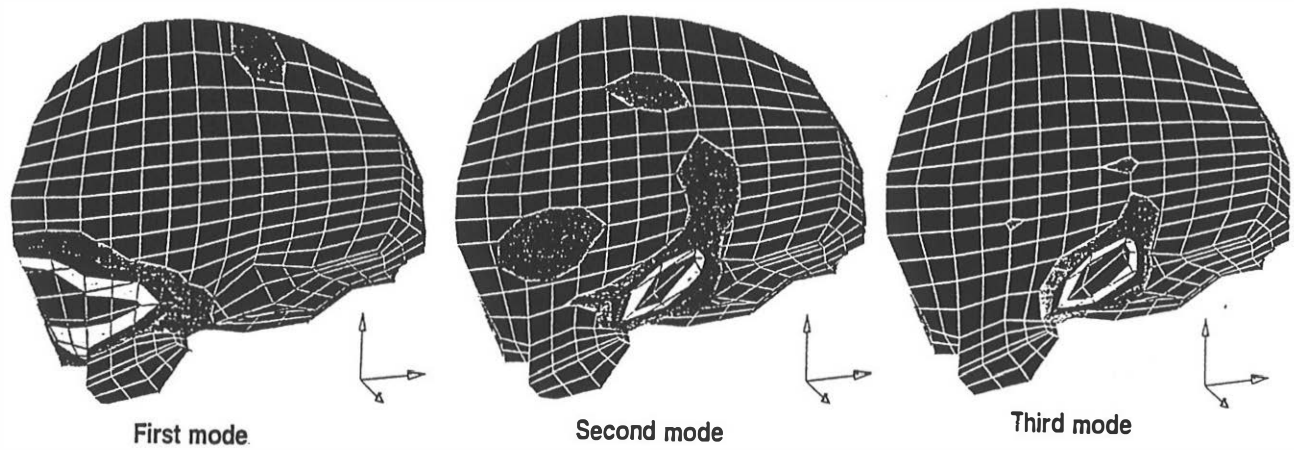

Fig.10 Strain energies of the first three mode shapes of the human brain

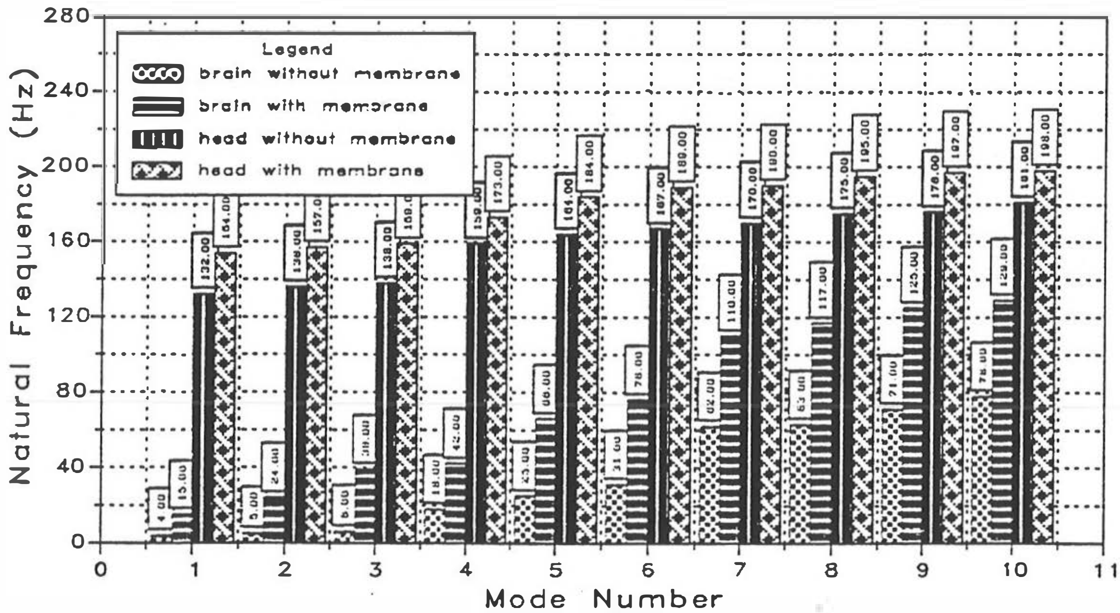

Fig.11 Frequencies of the human head and brain with and without membranes

In comparing with testing data, the frequencies from the baseline model are lower than those of Gurdjian et al (1970) who reported the first three frequencies of the living head to be 300, 560, and 920 Hz; and that of cadaver skull filled with gel to be 313, 600, and 800 Hz. Stalnaker et al (1971) reported that the natural frequency of the human cadaver head ranged from 166 to 820 Hz and that of monkey from 300 to 800 Hz. Willinger and Cesari (1990) found that the natural frequency of the human head was from 100 to 200 Hz. Tzeng et al (1993) identified the natural frequency of living head as ranging from 125 to 225 Hz for the first mode, 350 to 394 for the second mode, and 565 to 625 for the third mode, from seven healthy young male volunteers. The first natural frequency in this study is very comparable to that of measured by Stalnaker et al (1971), Willinger and Cesari (1990), and Tzeng et al (1993).

The interior membranes (dura and falx) affected the natural frequency of the brain as well as that of the full head. The frequency bar chart of the brain and the full head with and without membranes in Figure 11 shows these differences. The difference in brain frequency with and without membrane is much greater at low mode shapes than at the high ones (1.6 to 3.7 times from tenth mode to first mode). The difference in head frequency with and without the membranes was about 10%. The interior membranes tend to stiffen the cranial soft tissue and thus play a major rule in protecting the soft brain (Ruan et al, 1991).

DISCUSSION

Although modal analysis of the human head is based on the linear superposition principle and does not deal with a specific dynamic loading, its results are intrinsic or structure-born and hence can be used to predict the effects of applying various dynamic loads. Relative strains, internal loads, and stresses develop when the head deforms in a mode shape. These modal quantities, based on the relative displacement of a given mode shape, can be used to identify problem areas by identifying the more highly stressed elements, though they cannot be used to compare from one mode to another. Elements that are consistently highly stressed across many or all modes will probably be highly stressed when dynamic loads are applied. Since large strain energy (hence highly stressed) was shown in the base of the skull and brain stem, occipital lobe, and corpus callosum areas for most of the mode shapes, these areas are structurally weak in a free vibration mode.

When the head is freely vibrated, there are no local modes associated with the first, second, and third mode shapes (low frequency), as if the head moves like a solid body, but for the fourth and up to tenth mode shapes, local modes (hence local deformations) appear as if there is a decoupled or separation between head components such as the skull and brain. This is probably why some investigators have hypothesized that below a frequency of 150 Hz the head moves essentially as a rigid (solid) body (Gurdjian et al, 1970) and the skull and brain decoupled, allowing relative motion beyond a frequency of 200 Hz (Willinger and Cesari, 1990,1991). In fact, the head deforms in a mode shape, and high strain energies were shown **across** the inner table and the brain in the highly deformed areas for all ten modes. This indicates no separation between the skull and the brain. The "decoupled theory," based on the observation of a "plastic box + bovine brain + water + metallic support" test, may not be applied to the human cranial system. Using a lumped-spring-mass model (Willinger and Cesari, 1990) to decouple the mass of the brain (cerebral mass) and skull (frontal bone mass) to prove this decoupled theory may mislead and not accurately indicate brain-skull relative motion. Since modal analysis is based on the linear superposition principle and does not specify dynamic loadings, it cannot be applied to a nonlinear situation of general impact modes. The relative motion or separation (if any) between the skull and brain cannot be concluded from modal quantities.

Previous studies have shown that the brain exhibits less strain in short duration impacts than in long duration impact (Ruan and Prasad, 1995). Due to the incompressibility of the brain-CSF system, a general separation of the brain from the skull may be very unlikely during impact (Ueno et al, 1995). These studies are contrary to the decoupled theory. If we convert each frequency to impact duration using:

$$\tau = \frac{1}{2}T = \frac{1}{2}\frac{2\pi}{\omega_n} = \frac{\pi}{\omega_n}$$

where, τ = impact duration,
T = period,
ω_n = natural frequency, then

the equivalent impact durations for the skull, from mode 10 (high frequency) to mode 1 (low frequency), are 1.45 to 10 ms and that for the full head are 16 to 20 ms.

The brain possesses a very low frequency response. When testing the mechanical property of the brain experimentally with isolated brain tissue, the frequency sensitivity of the device used to obtain test data should be kept in the brain frequency range; otherwise, accurate test data may be difficult to acquire or missed entirely due to the frequency difference between the isolated brain tissue and the data acquisition system.

CONCLUSIONS

A finite element human head model has been used to carry out modal analysis of the cranial system. Frequencies of ten fundamental modes were extracted for the isolated skull condition with different element types and thicknesses; for the isolated brain with and without interior membranes; for the full head; for the full head with various CSF layer properties; and for the head-neck complex. The following conclusions can be drawn from this study.

1. The base of the cranium, brain stem, occipital lobe, and occipitotemporal areas are structurally weak in a free vibration mode.
2. Element type and thickness of the skull have significant effects on the skull natural frequency for the first two modes, but less effect was shown for the third to tenth modes. Whether the use of solid or shell elements is more appropriate to simulate the skull cannot be determined by modal analysis. Further study is needed to specify different loading conditions.
3. The material properties of the CSF layer do not significantly affect the frequency response of the head.
4. The neck restraint significantly influences the natural frequency response of the head for the first two modes, but less effect was shown for the third to tenth modes.
5. No local mode occurred in the first three mode shapes. Local modes only appeared in the fourth to tenth mode shapes for the skull.
6. Relative motion or separation between the skull and brain cannot be proven by a modal analysis since it did not deal with specific dynamic loadings. Further investigation is needed before we can address this question.

ACKNOWLEDGMENT

The authors would like to thank Mr. Roger Daniel for his critical review of the manuscript.

REFERENCES

Engin, A. E., and Liu, Y. K., "Axisymmetric Response of a Fluid-filled Spherical Shell in Free Vibrations," J. Biomech., Vol. 3, 1970, pp. 11-22.

Gurdjian, E. S., Hodgson, V. R., and Thomas, L. M., "Studies on Mechanical Impedance of the Human Skull: Preliminary Report," J. Biomech., Vol. 3, 1970, pp. 239-247.

Khalil, T. B., and Viano, D. C., "Experimental Analysis of the Vibrational Characteristics of the Human Skull," J. of Sound and Vibration, Vol. 63, 1979, pp. 351-376.

Misra, J. C., and Chakravarty, S., "A Free-vibration Analysis for the Human Cranial System," J. Biomech., Vol. 15, 1982, pp. 635-645.

Nickell, R. E., and Marcal, P. V., "In-Vacuo Modal Dynamic Response of the Human Skull," J. of Engineering for Industry, Vol. 3, 1974, pp. 490-494.

Ruan, J. S., Khalil, T. B., and King, A. I., "Human Head Dynamic Response to Side Impact by Finite Element Modeling," ASME Journal of Biomechanical Engineering, Vol. 113, 1991, pp. 276-283.

Ruan, J. S., Khalil, T. B., and King, A. I., "Finite Element Modeling of Direct Head Impact", *Proc. 37th Stapp Car Crash Conf.*, 1993, SAE Paper No. 933114.

Ruan, J. S., and Prasad, P., "Head Injury Potential Assessment in Frontal Impact by Mathematical Modeling," *Proc. 38th Stapp Car Crash Conf.*, 1994, SAE Paper No. 942212.

Ruan, J. S., and Prasad, P., "Coupling of a Finite Element Human Head Model with a Lumped Parameter Hybrid III Dummy Model - Preliminary Results," Journal of Neurotrauma, Vol. 12, Number 4, 1995, pp. 725-734.

Stalnaker, R. L., Fogle, J. L., and McElhaney, J. H., "Driving Point Impedance Characteristics of the Head," J. Biomech., Vol.4, 1971, pp. 127-139.

Tzeng, H. C., Tzeng, S. W., and Lee, M. C., "Vibrational Characteristics of the Human Head," AMD-Vol.169/BED-Vol.25, Crashworthiness and Occupant Protection in Transportation Systems, 1993, pp. 177-181.

Ueno, K., Melvin, J. W., Li, L., and Lighthall, J. W., "Development of Tissue Level Brain Injury Criteria by Finite Element Analysis," Journal of Neurotrauma, Vol. 12, Number 4, 1995, pp. 695-706.

Ward, C. C., and Thompson, R. B., "The Development of a Detailed Finite Element Brain Model," *Proc. 19th Stapp Car Crash Conf.*, 1975, SAE Paper No. 751163.

Willinger, R., and Cesari, D., "Determination of Cerebral Motion at Impact Through Mechanical Impedance Measurement," *Proceedings of the 1990 International IRCOBI Conference on the Biomechanics of Impacts, 1990, pp. 940-947.*

Willinger, R., and Cesari, D., "Brain Tolerance in the Frequency Field," Proceedings of 13th International Technical Conference on Experimental Safety Vehicles, 1991, pp. 940-947.

Willinger, R., Kopp, C. M., and Cesari, D., "New Concept of Contrecoup Lesions: Modal Analysis of a Finite Element Head Model," *Proceedings of the 1992 International IRCOBI Conference on the Biomechanics of Impacts, 1992, pp. 283-297.*

Willinger, R., Kopp, C. M., Ramet, M., Bouquet, R., and Caire, Y., "Proposition of A New Dummy Head: the Bimass 150 Principle," *Proceedings of the 1993 International IRCOBI Conference on the Biomechanics of Impacts, 1993, pp. 229-240.*

Willinger, R., Tableb, T., and Pradoura, P., "Head Biomechanics: From the Finite Element Model to the Physical Model," *Proceedings of the 1995 International IRCOBI Conference on the Biomechanics of Impacts, 1995, pp. 245-259.*